Tropical cloud-top height distributions revealed by the Ice, Cloud, and Land Elevation Satellite (ICESat)/Geoscience Laser Altimeter System (GLAS)

A. E. Dessler,[1] S. P. Palm,[2] and J. D. Spinhirne[3]

Received 23 September 2005; revised 20 January 2006; accepted 17 March 2006; published 30 June 2006.

[1] We analyze cloud-top height data obtained at tropical latitudes between 29 September and 17 November, 2003, from the Geoscience Laser Altimeter System (GLAS), carried onboard the Ice, Cloud, and Land Elevation Satellite (ICESat). About 66% of the tropical observations show one or more cloud layers. Of those observations that do show a cloud, about half show two or more cloud layers. Maxima in the cloud-top height distribution occur in the upper troposphere, between 12 and 17 km, and in the lower troposphere, below about 4 km. A less prominent maximum occurs in the midtroposphere, between 6 and 8 km. The occurrence of cloud layers tends to be consistent with the well-known diurnal cycles of continental and oceanic convection, and we find that cloud layers tend to occur more frequently over land than ocean, except in the lower troposphere, where the opposite is true. A particular emphasis of this paper is the convection that penetrates into the so-called tropical tropopause layer (TTL). We find more frequent occurrence of thick clouds in the TTL and above the tropopause than other studies, with 3.0% and 19% of the thick and thin cloud observations, respectively, showing a cloud top in the TTL and 0.34% and 3.1% showing a cloud top above the average level of the tropopause. These values are higher than those found in other data sets and suggest that an upward revision of TTL cloud frequency might be necessary. TTL clouds are observed more frequently in the evening than in the morning and more frequently over land than over ocean.

Citation: Dessler, A. E., S. P. Palm, and J. D. Spinhirne (2006), Tropical cloud-top height distributions revealed by the Ice, Cloud, and Land Elevation Satellite (ICESat)/Geoscience Laser Altimeter System (GLAS), *J. Geophys. Res.*, *111*, D12215, doi:10.1029/2005JD006705.

1. Introduction

[2] Clouds play a central role in the general circulation of the atmosphere, both through release of latent heat during their formation and through their regulation of incoming solar and outgoing longwave radiation. Despite the importance of clouds, however, there is still much that we do not know about them. In this paper, we analyze cloud-top heights measured by the Geoscience Laser Altimeter System (GLAS), carried onboard the Ice, Cloud, and Land Elevation Satellite (ICESat) in order to get a better picture of the horizontal and vertical distribution of tropical clouds.

[3] The GLAS is a diode-pumped Q-switched Nd:YAG laser operating in the near infrared (1064 nm) and visible (532 nm). Measurements of attenuated backscatter from the instrument are processed by the GLAS science team to produce high-quality measurements of cloud properties over much of the globe [*Spinhirne et al.*, 2005; *Zwally et al.*, 2002].

[4] During the period analyzed in this paper, 29 September to 17 November 2003 (referred to as the "laser-2a" period), the satellite obtained measurements at tropical latitudes in the morning and evening. Morning observations occurred between 6:58 am and 8:17 am, in daylight, with solar zenith angles ranging from 53° to 85°. Evening observations occurred between 6:58 pm and 8:17 pm, at night, with solar zenith angles ranging from 95° to 128°. While some information about the diurnal cycle can be obtained from these data, GLAS clearly does not provide a complete view of the diurnal cycle of cloud occurrence. This is a fundamental limitation of the data set.

[5] The data analyzed in this paper are based on GLAS' 532-nm data. The 532-nm channel of GLAS employs four Single Photon Counting Modules (SPCMs), which are sampled at 1.953 MHz, translating to a vertical resolution of 76.8 m. In this paper, we use the "high-resolution" cloud tops identified in the release 19 GLA09 data product [*Hart et al.*, 2005; *Palm et al.*, 2002], which are retrieved from an average of eight laser pulses occurring over 0.2 seconds. The satellite moves about 1.4 km over this time interval, and this distance defines the horizontal scale of features we are

[1]Department of Atmospheric Sciences, Texas A&M University, College Station, Texas, USA.
[2]Science Systems and Applications Inc., Lanham, Maryland, USA.
[3]NASA Goddard Space Flight Center, Greenbelt, Maryland, USA.

Copyright 2006 by the American Geophysical Union.
0148-0227/06/2005JD006705

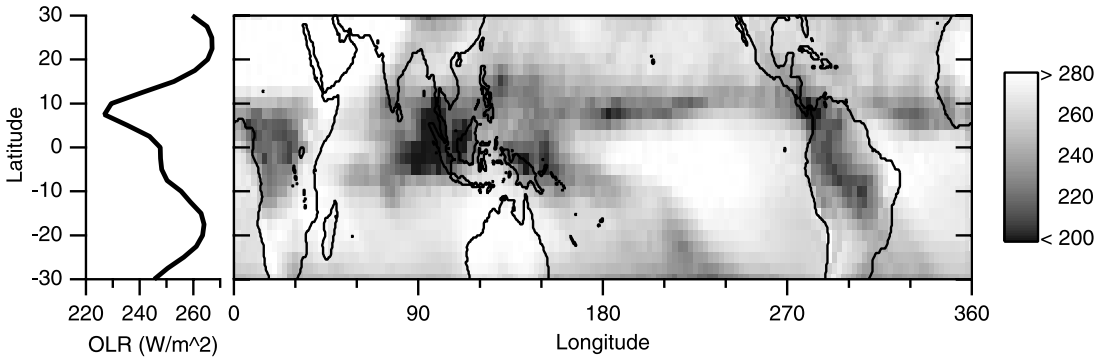

Figure 1. Outgoing longwave radiation (OLR) in W/m^2 averaged over the laser-2a period (29 September to 17 November 2003). The left panel is the zonal average, and the right panel is the latitude-longitude distribution. Calculated from daily NOAA/National Centers for Environmental Prediction/ Climate Prediction Center OLR.

investigating. A cloud top is defined as that height where the first of two consecutive GLAS data bins of 76.8 m (from above the cloud moving downward) exceed a threshold based on molecular scattering; the bottom is that height where the first of two consecutive bins are less than the threshold (from within the cloud moving downward). GLAS can detect clouds with optical depths down to about 0.002 at night, but the ability to detect clouds drops off rapidly below 0.02 during the day [*Hlavka et al.*, 2005; *Palm et al.*, 2002]. The design of the 5-Hz cloud detection algorithm is such that relatively thin (optical depth < 0.2) clouds less than 5–6 km in horizontal extent may go undetected. This is caused by the horizontal averaging of data to a resolution of 28 km before cloud detection begins to reduce signal noise. We believe that the oversight of such clouds will introduce errors of approximately 1 percent or less in our cloud frequencies.

[6] The inherent uncertainty of the cloud-top height is equal to the SPCM resolution of 76.8 m. In addition, GLAS measurements of cloud altitude are made with respect to the geoid, an equipotential surface of the Earth's gravity field that most closely approximates mean sea level (MSL). Differences between the geoid and MSL can be as much as a few tens of meters. Combining all of the sources of uncertainty produces a total uncertainty in cloud height above MSL of less than 100 m. For a thorough discussion of the GLAS data, see the special section papers on ICESat/ GLAS atmosphere data in *Geophysical Research Letters*, *32*(21,22), 2005.

[7] In this paper we compare the GLAS results with other cloud climatologies. Such comparisons must be done with care, however, because different methods of inferring cloud-top height can produce quite different statistics for exactly the same cloud population. For example, one common way to measure cloud height is with a precipitation radar. This type of radar responds primarily to precipitation-sized particles, while the GLAS 532-nm lidar responds to both precipitation-sized and smaller particles. During the growing phase of convective clouds, it is likely that the cloud tops observed by radar and lidar are roughly coincident. On the other hand, during the decaying phase of the same convective event, the two tops may differ significantly. Likewise, for other cloud types (e.g., nimbostratus, cirrus) the correlation between radar-echo top and GLAS cloud top can be poor.

[8] Another common way to measure cloud height uses measurements from nadir-viewing passive infrared radiometers. These instruments measure upwelling infrared radiance emitted from about one optical depth below the cloud top, and convert this to a cloud-top height. The most common way of converting radiance to cloud-top height is by finding the height in a nearby temperature profile where the environmental temperature equals the cloud-top brightness temperature, and assigning that height to the cloud top (for clouds with optical depths below one, more sophisticated methods, such as CO_2 slicing [*Wylie and Menzel*, 1989], must be used). GLAS, on the other hand, detects a cloud top at the point where the optical depth, measured from the top of the cloud downward, exceeds an optical depth of 0.002–0.02. Just as for radars, it has been assumed that these two levels are near each other for thick, convective clouds because of the high ice water content of deep convective clouds. However, case studies using aircraft data [e.g., *Heymsfield et al.*, 1991; *McGill et al.*, 2004] have shown that the one optical depth level can sometimes lie several kilometers below the lidar-detected cloud top, and a recent study [*Sherwood et al.*, 2004] found that this distance was typically 1 km even for deep convective clouds.

[9] In addition, the conversion to height using a nearby temperature profile also introduces uncertainty. *Sherwood et al.* [2004] compared infrared cloud-top heights derived using this method with lidar-estimated heights of the one optical depth level and found an unexplained offset of $\sim$1 km in deep convective clouds. Thus there might be a 2-km or larger offset between the cloud tops from the GLAS and infrared-based climatologies.

2. Vertical Distribution of Clouds

[10] From a meteorological perspective, the latitude of the "tropics" shifts throughout the year, approximately following the annual latitudinal migration of the Sun. Figure 1 shows the average outgoing longwave radiation (OLR) during the laser-2a period (based on the NOAA Interpolated OLR data set [*Liebmann and Smith*, 1996]). Low values of

OLR are a proxy for deep convection, and the OLR data show relatively confined minima over equatorial Africa and South America, as well as a broad minimum over the Western Pacific. Also evident are the intertropical convergence zone and the South Pacific convergence zone. Overall, most of the deep convection during this time period is found between 10°S and 20°N, with significant longitudinal variation. As a result, we will focus in this paper on the latitude range 10°S to 20°N, and we will average over this latitude range to construct "tropical" averages.

[11] During the laser-2a period, the GLAS made 3.46 million observations evenly distributed over the latitude range 10°S–20°N (each 1° × 1° box in the tropics contains 150–500 GLAS measurements obtained over about 4–5 days distributed throughout the laser-2a period). GLAS detected at least one cloud layer in 2.27 million or 66% of the measurements, while 1.18 million or 34% observed no clouds. Of the GLAS observations that detect at least one cloud layer, about half detected two or more layers. In total, GLAS observed 3.47 million cloud layers.

[12] In our analysis, GLAS observations are divided into "thick" and "thin" cloud layers. Following *Heymsfield and McFarquhar* [1996], we define "thick" clouds to be those that extinguish the lidar's laser beam: meaning that there are no reflections from lower cloud layers or the surface. In the absence of multiple scattering, the GLAS lidar would be totally attenuated by clouds with an optical depth of 2.0–2.5. Multiple scattering, however, allows photons to penetrate more deeply into clouds, with the exact effects of multiple scatter being dependent on cloud particle size, cloud height, and optical depth. Figure 9 of *Duda et al.* [2001] shows that on average multiple scattering would increase cloud transmission by a factor of 1.5–2.0, with a maximum effect of a factor of about 3 for low clouds with particle sizes in the 10–20 micron range. Therefore, on average, thick clouds have optical depths greater than about 4 [see also *Spinhirne and Hart*, 1990], but may occasionally penetrate to an optical depth of 6–7.

2.1. Geometric Altitude

[13] In Figure 2 we plot the cloud-top height distribution of thick (solid line) and thin (dotted line) cloud layers on nine panels, with the data broken down by surface type and time of measurement. Figure 2 shows that there are two main peaks in the cloud-top distribution: in the upper troposphere (UT), between 12 and 17 km, and in the lower troposphere (LT), below about 4 km. In general, the thick and thin distributions show peaks at the same altitude and have approximately the same shape, although there are generally fewer thick clouds.

[14] We calculate the cloud-top fraction at a particular height by dividing the number of cloud tops observed at that height by the number of GLAS observations where the laser penetrated to that height. We determine that the laser penetrated to a given height if either the ground or a cloud layer at a lower altitude is detected. As one goes deeper into the atmosphere, the number of GLAS observations that reach a particular altitude decreases because of extinction of the laser by overlying clouds. This method produces the correct cloud fraction if clouds at different levels of the atmosphere are uncorrelated — in other words, if clouds occur at an altitude with equal probability whether an overlying thick cloud exists or not. This is a well-known approach that has been applied previously to Stratospheric Aerosol and Gas Experiment (SAGE) II and International Satellite Cloud Climatology Project (ISCCP) cloud climatologies [*Wang et al.*, 1995; *Bergman and Salby*, 1996].

[15] We could have assumed that clouds never occur beneath thick clouds. Had we assumed that, our calculated cloud fractions would have been essentially unchanged in the UT, and about 20–25% lower in the LT. Alternatively, we could have assumed that clouds occur more frequently beneath thick clouds. Once again, this would lead to little change in the UT. The effect in the LT can be estimate as follows. About 20% of the GLAS observations see a thick cloud in the UT; if a cloud occurred in the LT beneath every one of these thick clouds, it would about double the occurrence in the LT compared to our random-cloud assumption. The behavior of overlapping thick clouds is, in the end, a fundamental uncertainty of this data set.

[16] The vertical distribution of clouds in the "all data" panel is similar to the vertical distribution derived from SAGE II data by *Wang et al.* [1995, Figure 1]. Between 7 and 18 km, the integrated cloud fractions are in good agreement, with values for GLAS (thick plus thin) and SAGE II of 65% and 60%, respectively. Between 2 and 7 km, however, the agreement is poorer, with integrated cloud fractions of 21% and 60%. The GLAS frequency is lower than the SAGE II frequency throughout the 2–7 km altitude range, but the majority of the integrated disagreement is due to a large difference around 2 km.

[17] There are several aspects of the comparison that make quantitative conclusions difficult to draw. The most important problem is that the two instruments have vastly different viewing geometries. SAGE II is a limb-viewing instrument and measures the integrated horizontal optical depth of the clouds, while GLAS views the nadir and measures the optical depth in the vertical. Because of this, it is possible for either GLAS or SAGE II to detect a cloud that the other one misses. A second potential explanation is that the horizontal area of a SAGE II measurement (200 × 2.5 km^2) is about five thousand times larger than the horizontal area of a GLAS measurement (70 m × 1.4 km). Increasing the horizontal coverage of a measurement increases the chance of encountering a cloud, thus providing a potential explanation for the much larger fraction of boundary-layer clouds observed by SAGE. See the work of *Liao et al.* [1995] for a thorough discussion of these potential biases. Finally, some of the difference might also be due to differing time periods (the SAGE II distribution is based on an annual average of data obtained in 1986, while the GLAS distribution is based on data are from the 6-week laser-2a period).

[18] The Lidar In-Space Technology Experiment (LITE) made measurements for 53 hours during a flight of the space shuttle in September 1994, and has detection characteristics similar to GLAS. *Winker and Trepte* [1998] reported "laminar" cirrus (cloud tops > 15 km, thickness < 1 km) in about 14% of their nighttime tropical observations between 20°S and 30°N. GLAS sees such clouds in 11% of its observations over this same latitude range. Given differences in the time of the two data sets, as well as the sparse and uneven sampling of the LITE data set, the agreement between these two data sets appears good.

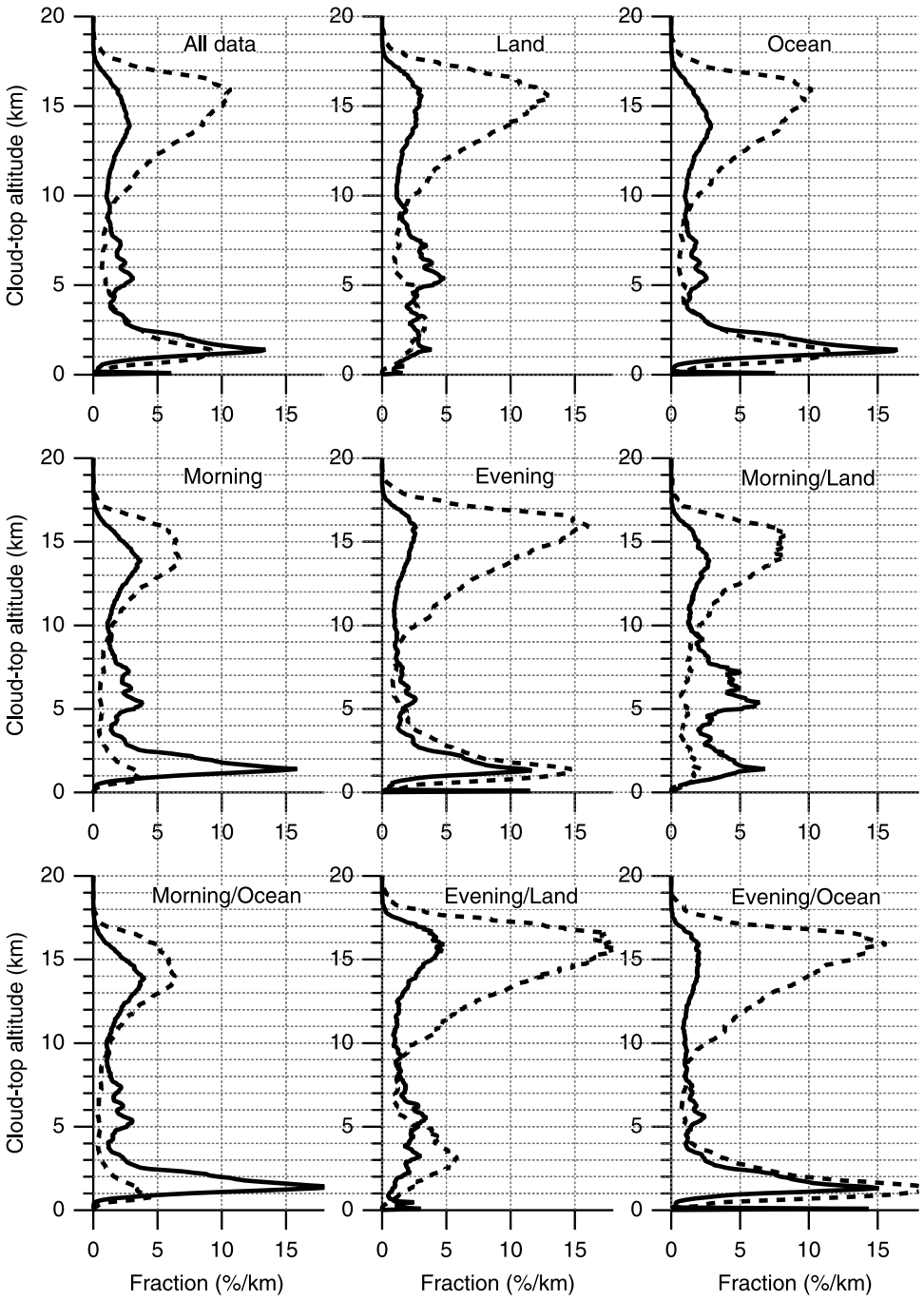

Figure 2. Fraction of GLAS observations (percent per km) between 10°S and 20°N that contain a cloud-top versus altitude (km). The solid lines are for thick clouds, and the dashed lines are for thin clouds. The histogram has been constructed using bins of 76.8 m, the native resolution of the GLAS data.

[19] Because there are many more thin than thick clouds, the details of the thick cloud-top distribution are difficult to see on Figure 2. To remedy this, in Figure 3 we plot the thick cloud-top height distribution alone. These thick-cloud distributions show peaks in the UT and LT, just like the thin-cloud distributions, and also often show a smaller maximum in the midtroposphere, peaking at 6–8 km.

[20] *Johnson et al.* [1999] previously identified this trimodal distribution in thick, precipitating clouds: a bottom layer, peaking between 1 and 2 km, corresponding to boundary layer cumuli; a midlevel layer, peaking at about 6 km, corresponding to shallow convection; and an upper layer, peaking around 15 km, corresponding to deep cumulus convection. *Johnson et al.* [1999] used data exclusively from ocean measurements in the Western Pacific. We show here that the trimodal distribution is generally apparent in the global GLAS thick-cloud data, although far less obvious in the thin-cloud data. *Johnson et al.* [1999] pointed out that these peaks in cloud-top frequency are in close proximity to prominent stable layers in the atmosphere: the trade stable

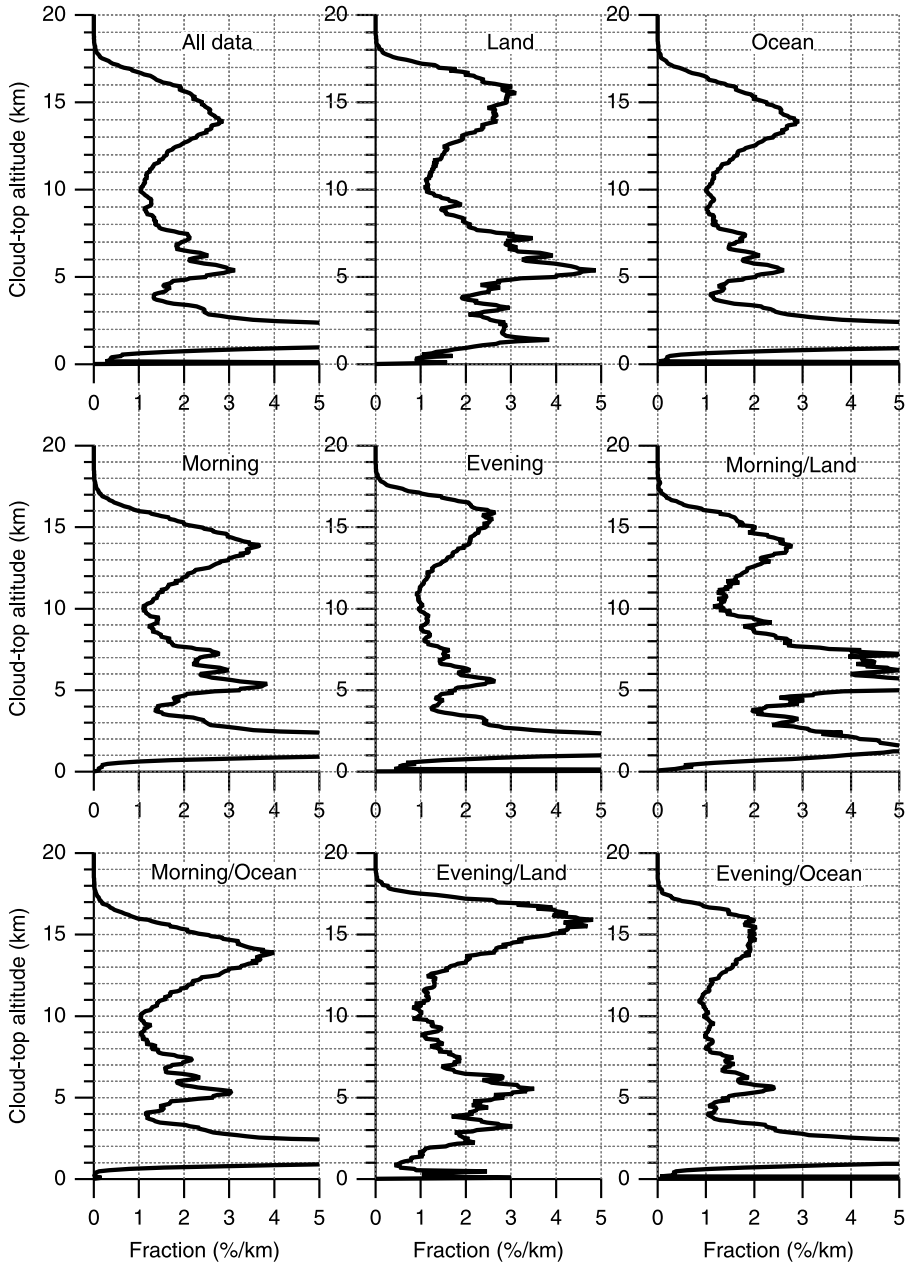

Figure 3. Same as Figure 2 but for thick clouds only.

layer around 2 km, the 0°C melting level around 5 km, and the tropopause layer beginning around 15 km. *Folkins and Martin* [2005] have presented a simple model that also explains this arrangement of clouds.

[21] Figures 2 and 3 are summarized in Tables 1 and 2, which give the cloud frequency integrated over various height ranges for thick and thin clouds, respectively. The top row of both tables contains the fraction of cloud-layer tops above 16.5 km, a typical tropopause altitude. The second row contains the fraction above 14.5 km, which is the typical level of the base of the so-called tropical tropopause layer (discussed below). The third row contains the fraction above 10 km, a typical lower boundary for the UT; the fourth row contains the fraction in the midtroposphere, between 4 and 10 km; the fifth contains the fraction in the boundary layer, below 4 km; and the sixth contains the total cloud occurrence at all altitudes. The bottom row of Table 1 contains the total number of GLAS observations in each category (in thousands), and can be used to convert the fractions in Tables 1 and 2 to actual cloud numbers. Note that the total number of thin cloud tops in Table 2 exceeds 100% in some categories. This is not an error, but reflects the fact that a significant fraction of GLAS observations contain more than one cloud.

[22] Table 1 shows that the frequency of thick cloud layers is nearly the same in the morning and evening, with slightly more thick cloud layers in the evening above 14.5 km, and slightly fewer below. Table 2 shows that thin cloud layers are more frequent in the evening than in the morning at all altitudes.

Table 1. Thick Cloud-Top Occurrence Integrated Over Geometric Altitude Ranges, Expressed as a Fraction of Total GLAS Observations[a]

	All Data	Morning	Evening	Land	Ocean	Land/Morning	Land/Evening	Ocean/Morning	Ocean/Evening
z > 16.5 km	0.69	0.20	1.2	1.5	0.44	0.16	2.9	0.21	0.66
z > 14.5 km	4.7	3.5	5.9	6.9	4.0	3.0	11.0	3.6	4.4
z > 10 km	13.1	14.0	12.1	14.8	12.5	11.6	18.1	14.8	10.3
10 > z > 4 km	10.8	12.6	9.0	16.1	9.1	20.5	11.5	10.1	8.2
z < 4 km	18.1	19.5	16.8	9.3	20.9	12.2	6.5	21.8	20.0
All altitudes	41.9	46.1	37.9	40.1	42.5	44.3	36.1	46.7	38.5
GLAS observations	3457	1729	1729	842	2615	421	421	1308	1308

[a]Values are given in percent. The bottom row shows the total Geoscience Laser Altimeter System (GLAS) observations in each category (in thousands).

[23] One confounding aspect of this thin cloud morning-evening comparison is that GLAS can detect clouds with optical depths down to about 0.002 at night, while GLAS' ability to detect clouds during sunlit conditions drops off rapidly below 0.02 [*Hlavka et al.*, 2005; *Palm et al.*, 2002]. This will have little effect on measurements of thick clouds, but it means that GLAS will observe more thin clouds in the evening than in the morning, even if there were no actual change in the number of clouds.

[24] We can investigate this uncertainty using GLAS measurements of optical depth, which are reported at medium resolution (1 Hz) in the release 19 GLA11 product. These data suggest that about one-third of the diurnal cycle of thin cloud layers seen in the GLAS medium-resolution cloud data are contributed by evening observations of clouds with optical depths below 0.02. We conclude that the morning-evening differences identified in the high-resolution GLAS data do reflect an actual change in the number of clouds, but the magnitude of the difference seen in Table 2 likely overestimates the actual difference. Clearly, this is another fundamental uncertainty of the GLAS data set.

[25] The strong tendency in the GLAS data for UT cloud layers over land to occur more frequently in the evening than in the morning is likely associated with the diurnal cycle of continental deep convection, which is well known to peak in the afternoon and evening (*Bergman and Salby* [1996], *Nesbitt and Zipser* [2003], *Wylie and Woolf* [2002], *Yang and Slingo* [2001], *Alcala and Dessler* [2002], and many others). Over ocean, GLAS data show a similar tendency, but the magnitude is much smaller — consistent with a weaker diurnal cycle that reaches a maximum in the middle of the night [e.g., *Bergman and Salby*, 1996; *Nesbitt and Zipser*, 2003; *Alcala and Dessler*, 2002].

[26] Tables 1 and 2 also show that both thick and thin cloud layers are more frequent over land than over ocean, except for thick clouds below 4 km, which are more frequent over the ocean. Breaking down the observations by both surface type and time of day, thin cloud layers are more frequent in the evening than in the morning over both land and ocean. For thick cloud layers over land, there are more clouds observed in the evening above 10 km, and fewer below. Over ocean, there are more thick clouds in the evening above 14.5 km, and fewer below. The midlevel thick cloud layer peak occurs most frequently in the morning over land, with evening land, evening ocean, and morning ocean occurring about half as frequently.

[27] Finally, we note that land and ocean frequencies in this paper have been calculated by dividing cloud observations over land (ocean) by total observations over land (ocean). However, since ocean makes up 76% of the Earth's surface area between 10°S and 20°N, one must take this into account when comparing numbers of events rather than percentages. For example, while the frequency of thick cloud events at altitudes above 14.5 km over land (6.9%) is greater than the frequency over ocean (4.0%), the actual number of events over ocean is greater than those over land owing to the greater area of ocean.

2.2. Clouds in the Tropical Tropopause Layer

[28] A topic of particular interest in the scientific community is the so-called tropical tropopause layer (TTL), a transition layer between the troposphere and stratosphere [e.g., *Atticks and Robinson*, 1983; *Highwood and Hoskins*, 1998; *Folkins et al.*, 1999]. While various definitions exist for this layer, one oft-cited definition puts the bottom boundary at the level of zero net-radiative heating [*Sherwood and Dessler*, 2000, 2001], which occurs between 14.5- to 16-km altitude or 355- to 365-K potential temperature [*Folkins et al.*, 1999; *Gettelman et al.*, 2004]. The upper limit of the TTL is the level where overshooting convection tails off, around 18 km [e.g., *Alcala and Dessler*, 2002; *Gettelman et al.*, 2002b]. The tropopause lies within the TTL; various definitions of the tropopause also exist, but they generally put its location somewhere around 16.5–17 km (375- to 380-K potential temperature), about 1–2 km (15–25-K potential temperature) above the base of the TTL. Processes occurring in the TTL set the chemical composition of the air entering the stratosphere. Clouds in this region play a potentially important role in these processes

Table 2. Thin Cloud-Top Occurrence Integrated Over Geometric Altitude Ranges, Expressed as a Fraction of Total GLAS Observations[a]

	All Data	Morning	Evening	Land	Ocean	Land/Morning	Land/Evening	Ocean/Morning	Ocean/Evening
z > 16.5 km	5.7	1.4	10.1	8.4	4.9	1.7	15.3	1.3	8.4
z > 14.5 km	25.6	12.6	38.9	32.0	23.6	15.8	48.9	11.5	35.7
z > 10 km	49.9	31.2	68.8	59.7	46.8	37.6	82.9	29.1	64.5
10 > z > 4 km	6.4	4.6	8.0	9.5	5.4	7.6	11.3	3.7	7.1
z < 4 km	17.0	6.0	27.1	9.1	19.5	4.8	13.2	6.5	31.5
All altitudes	73.2	41.9	104.0	78.2	71.8	50.0	107.4	39.3	103.1

[a]Values are given in percent.

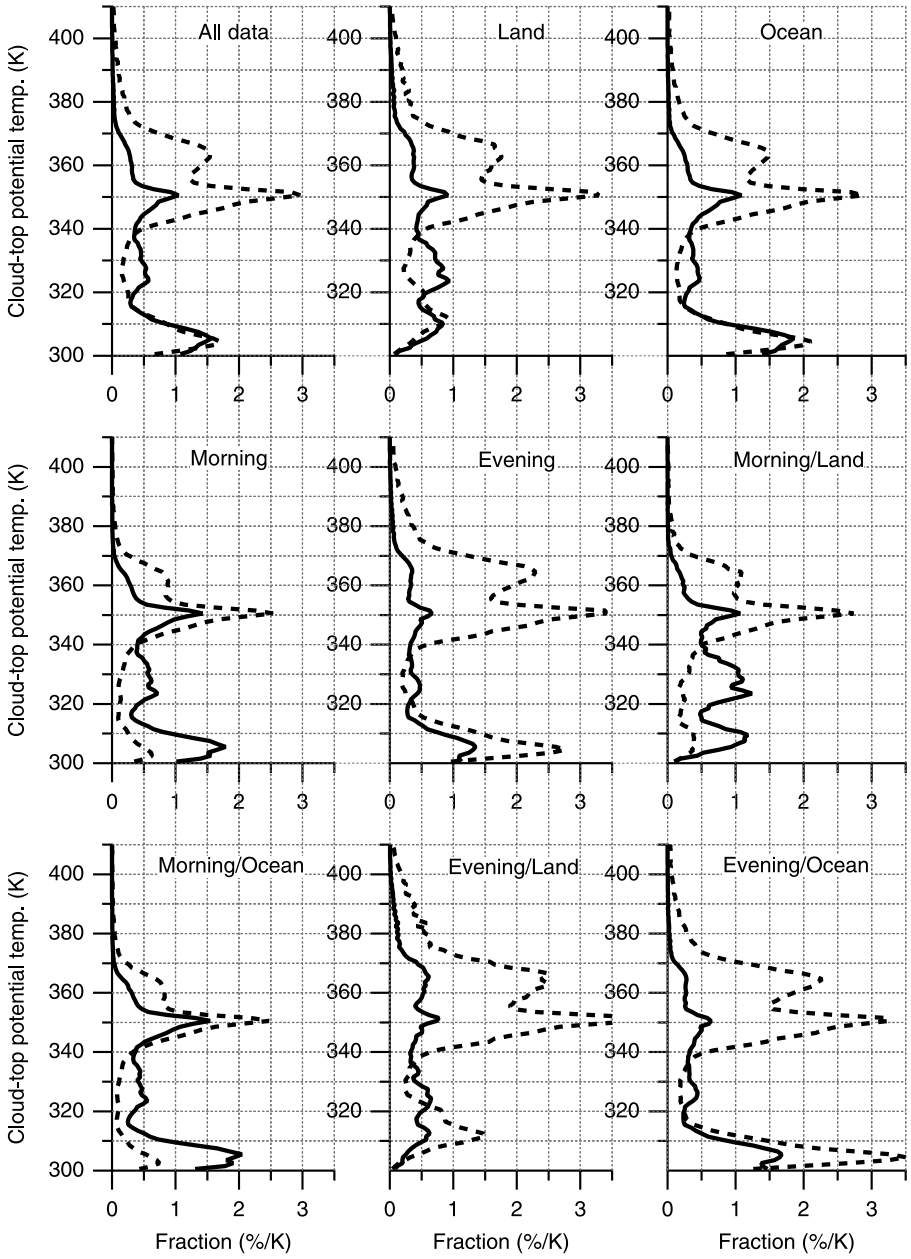

Figure 4. Same as Figure 2 but with potential temperature as the vertical coordinate.

[e.g., *Holton et al.*, 1995; *Sherwood and Dessler*, 2001; *Dessler*, 2002]. Thin (optical depth $\ll 1$) cirrus in the TTL are of particular interest to the scientific community. They are potentially radiatively important [e.g., *McFarquhar et al.*, 2000; *Hartmann et al.*, 2001; *Jensen et al.*, 1996] and potentially play a role in dehydration of air entering the stratosphere [e.g., *Holton and Gettelman*, 2001; *Gettelman et al.*, 2002a; *Jensen and Pfister*, 2004; *Luo et al.*, 2003]. TTL thin-cirrus measurements by GLAS are studied in detail by *Dessler et al.* [2006].

[29] For TTL studies, potential temperature is a more convenient coordinate than geometric altitude. Therefore in Figure 4 we plot the same data as in Figure 2 but as a function of potential temperature. To construct these plots, measurements of geometric altitude, the quantity measured by GLAS, are converted to potential temperature using assimilated meteorological data from the United Kingdom Meteorological Office (UKMO) [*Swinbank and O'Neill*, 1994], which is produced on a regular grid once per day. To calculate the potential temperature of each cloud top, we assume that geometric height above the geoid, which is measured by GLAS, and geopotential height, which is reported in the UKMO data set, are equivalent. We then use a geopotential height-potential temperature relation for the location of the GLAS measurement interpolated from the UKMO meteorological fields to determine the potential temperature at any height.

[30] This conversion introduces additional uncertainties. The assumption that geometric height equals geopotential height introduces an error of several tens of meters in

Table 3. Thick Cloud-Top Occurrence Integrated Over Potential Temperature Ranges Covering the TTL, Expressed as a Fraction of Total GLAS Observations[a]

	All Data	Morning	Evening	Land	Ocean	Land/Morning	Land/Evening	Ocean/Morning	Ocean/Evening
$\theta > 377.5$ K	0.34	0.07	0.61	0.87	0.17	0.06	1.7	0.08	0.26
$\theta > 360$ K	3.0	1.7	4.4	5.1	2.3	1.7	8.7	1.6	3.0
$\theta > 340$ K	13.7	14.7	12.7	15.4	13.2	12.2	18.6	15.4	10.9

[a]Values are given in percent. TTL, tropical tropopause layer.

the UT, corresponding to an error of a few tenths of a degree K of potential temperature. More significant are errors in the meteorological fields. Errors in the UKMO [*Randel et al.*, 2000] temperatures of 3 K in the TTL translate into an uncertainty in cloud potential temperature in the neighborhood of as much as 6 K. Another uncertainty is that using the once-per-day UKMO data misses diurnal variations of temperature and other variables. *Seidel et al.* [2005] estimate the diurnal variations of temperature in the UT and TTL are small, less than 1 K, which translates into an uncertainty in potential temperature of less than 2 K. Adding the uncertainties in quadrature, we estimate the total uncertainty in potential temperature to be ~7 K. We should also emphasize that our method determines the potential temperature of the local environment at the altitude of the cloud, not the actual potential temperature of the cloud air.

[31] Figure 4 shows most of the same general features as Figure 2, and we will therefore not repeat them here. Several new features, however, emerge in this coordinate system. In the UT, what Figures 2 and 3 shows to be a broad general peak from ~12–17 km is revealed to have a more complex structure. The most dominant feature of the UT is a strong but relatively narrow peak at 350 K. This peak is close in altitude to a climatological minimum in ozone mixing ratio associated with a maximum in convective detrainment [*Folkins et al.*, 2002].

[32] Importantly, the 350-K level is just below the zero net-radiative-heating line [*Folkins et al.*, 1999; *Gettelman et al.*, 2004]. Air detraining below this zero net-radiative-heating line will generally descend back to the surface as part of the overturning Hadley circulation. Thus Figure 4 shows that there is a strong tendency for cloud tops to occur just below this important level.

[33] Figures 2 and 3 show that the broad UT peaks for both thick and thin clouds move upward by a few kilometers between the morning and evening. The plots vs. potential temperature show that, for thick clouds, this general upward movement is caused by a decrease in the 350-K peak combined with growth of a peak at 365 K; for thin clouds, there is an increase in occurrence at both 350 and 365 K, but the growth at 365 K dominates, leading to an increase in average height. This 365-K peak is above the zero-net radiative heating line, suggesting that processes forming these clouds (such as deep convection) can have an impact on the abundance of constituents, especially water vapor, in the stratosphere. Thus, understanding the origin of this cloud peak is of practical importance to understanding the problem of troposphere-to-stratosphere transport.

[34] Tables 3 and 4 summarize Figure 4 by providing cloud frequency integrated over various potential temperature ranges in the UT. The top row contains the fraction of thick cloud tops above 377.5 K, which is the typical level of the tropopause. The second row contains the fraction above 360 K, which is the typical level of the base of the TTL. The third row contains the fraction above 340 K, which can be considered the bottom of the UT. Cloud-top frequencies in the TTL and above the tropopause are a factor of ~3–5 times higher than those obtained from radar [*Alcala and Dessler*, 2002] and passive infrared [*Gettelman et al.*, 2002b] methods. Such disagreements are consistent with previous analyses (see the discussion in section 1).

2.3. Horizontal Distribution

[35] Figure 5 shows the horizontal distribution of cloud tops in four potential temperature ranges: 365–375 K, within the TTL but just below the tropopause; 345–355 K, around the 350-K peak and just below the zero net-radiative-heating line; 315–340 K, in the midtroposphere; and below 315 K, containing boundary-layer clouds. In these figures we plot the probability that there is one or more clouds in the layer in the combined morning and evening and thick and thin data. The separate thick and thin distributions (not shown) display similar horizontal gradients.

[36] The cloud-top distributions in the top three potential temperature ranges show strong correlation with low OLR (Figure 1), a proxy for convection. In the UT, cloud occurrence is relatively confined to regions of low OLR. This correspondence was also displayed in the passive-infrared high-cloud data of *Wylie and Menzel* [1999], *Bergman and Salby* [1996], and *Gettelman et al.* [2002b], in the radar data of *Liu and Zipser* [2005] and *Alcala and Dessler* [2002], and in the limb-sounding SAGE II data of *Wang et al.* [1996].

[37] In the midtroposphere, cloud occurrence maximizes in regions of low OLR, but significant occurrence extends

Table 4. Thin Cloud-Top Occurrence Integrated Over Potential Temperature Ranges Covering the TTL, Expressed as a Fraction of Total GLAS Observations[a]

	All Data	Morning	Evening	Land	Ocean	Land/Morning	Land/Evening	Ocean/Morning	Ocean/Evening
$\theta > 377.5$ K	3.1	0.52	5.6	5.3	2.4	0.74	9.9	0.46	4.0
$\theta > 360$ K	18.7	7.8	29.9	24.4	16.9	10.5	38.9	6.9	27.0
$\theta > 340$ K	50.8	31.9	69.9	60.5	47.7	38.4	83.8	29.8	65.6

[a]Values are given in percent.

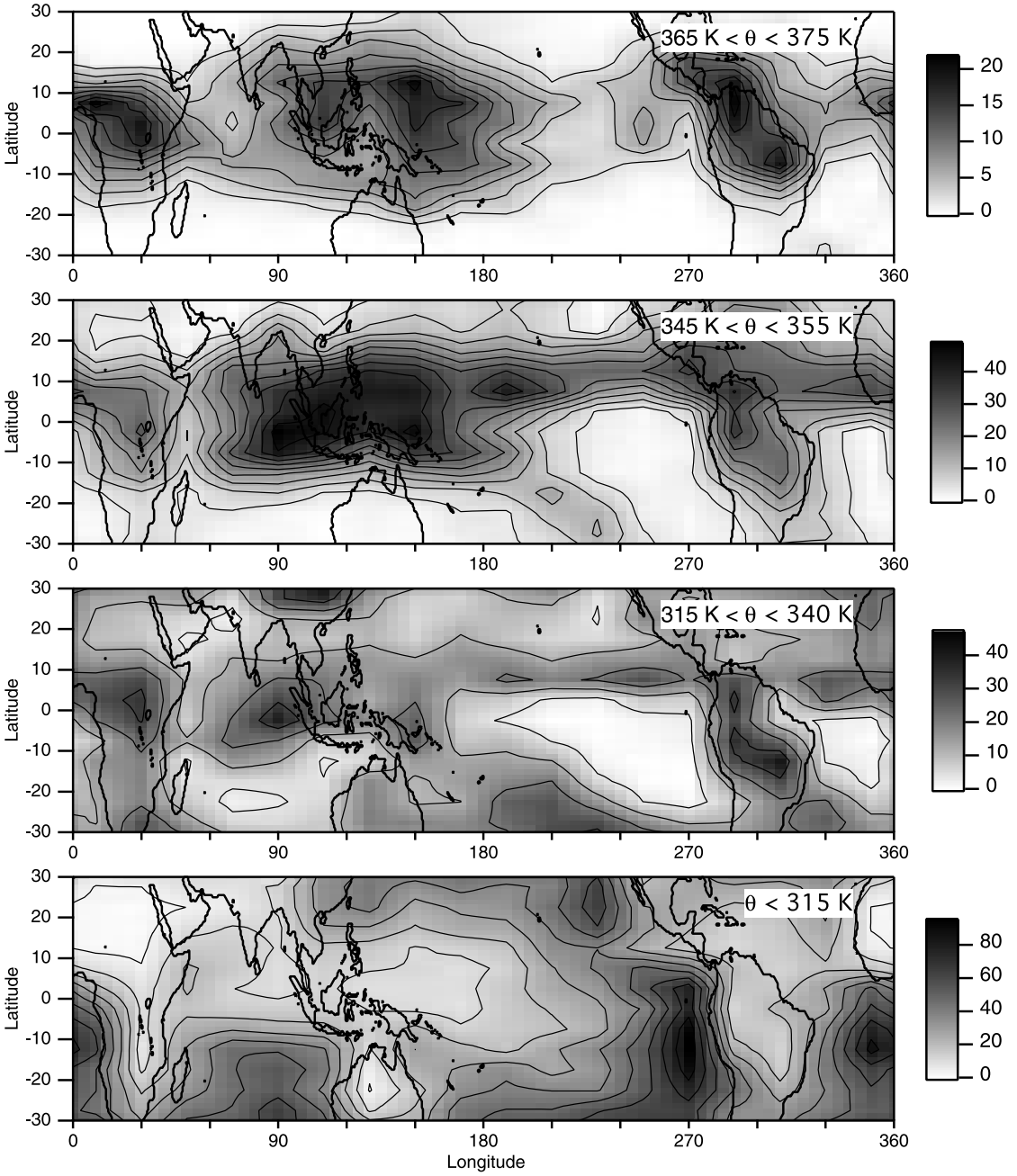

Figure 5. Fraction of GLAS observations (in percent) with at least one cloud in the specified potential temperature range. Plot includes both thick and thin clouds and both morning and evening data.

beyond the deep-convective regions. The lowest potential temperatures, corresponding to boundary-layer clouds, appears anticorrelated with convection — the exact opposite of higher-level clouds. *Bergman and Salby* [1996] analyzed ISCCP data and also found that the distribution of low clouds is approximately a mirror image of the distribution of high clouds. *Norris* [1998] also observed a similar tendency in synoptic surface cloud observations.

3. Conclusions

[38] In this paper we have analyzed tropical cloud-top heights from the Geoscience Laser Altimeter System (GLAS), carried onboard the Ice, Cloud, and Land Elevation Satellite (ICESat), obtained between 29 September and 17 November, 2003 (referred to as the "laser 2a" period). During this time, most convection was located between 10°S and 20°N, and we focused on that latitude range in this paper. Knowing the three-dimensional distribution of tropical clouds is of primary importance for understanding the role that clouds and their associated latent and radiative heating play in the Earth's general circulation. Further, feedbacks involving clouds are one of the more uncertain aspects of our predictions of climate change, and this data set can provide a baseline for research on this problem. Deep convective clouds also play a role in rapid, vertical

constituent transport from the lower to the upper troposphere, while clouds in the so-called tropical tropopause layer (TTL) play a role in dehydration of air entering the stratosphere, which has important implications for climate and stratospheric chemistry [e.g., *Dessler*, 2000].

[39] GLAS observed cloud layers in 66% of its observations between 10°S and 20°N. Of those observations that do show a cloud layer, about half show two or more clouds. Maxima in the cloud-top height distribution occur in the upper troposphere, between 12 and 17 km, and in the lower troposphere, below about 4 km. A less prominent maximum occurs in the midtroposphere, between 6 and 8 km, in agreement with previous analyses of a trimodal distribution of clouds [*Johnson et al.*, 1999].

[40] GLAS observations occur around 8 am and 8 pm local solar time and therefore provide limited information on the diurnal cycle of cloud frequency. We see that the frequency of thick cloud layers is nearly the same in the morning as in the evening, with slightly more thick cloud layers in the evening above 14.5 km, and slightly fewer below. Thin cloud layers are more frequent in the evening than in the morning at all altitudes, but the greater sensitivity of GLAS at night suggests that these data likely overestimate the morning-evening difference. We also looked at differences in cloud occurrence over land and ocean. Both thick and thin clouds occurred more frequently over land, except for thick clouds below 4 km, which occurred with greater frequency over the ocean.

[41] A particular emphasis of this paper has been convection that penetrates into the TTL. We find more frequent occurrence of thick clouds in the TTL and above the tropopause than other studies, with 3.0% and 19% of GLAS observation showing a thick and thin cloud top in the TTL, respectively, and 0.34% and 3.1% showing a thick and thin cloud top above the average level of the tropopause. Over both land and ocean, these clouds are observed more frequently in the evening than in the morning. These values are significantly higher than seen in other data sets of TTL clouds, and we attribute differences to the superiority of the lidar method for detecting thin clouds and in accurately determining cloud altitude.

[42] The horizontal distribution of clouds in the UT and midtroposphere tends to follow the distribution of convection, as might be expected. In the LT the distribution is the opposite, with low occurrence frequency in regions of convection.

[43] This analysis, while informative, has some severe limitations. Probably the most severe limitation is that the data set analyzed here is limited to one six-week period in late 2003. We look forward to analyzing other GLAS periods, as well as data from the upcoming Cloud-Aerosol Lidar and Infrared Pathfinder Satellite (CALIPSO), CloudSat, and Aura missions in order to gain a more thorough understanding of the distribution of cloud layers in the atmosphere.

[44] **Acknowledgments.** We would like to thank the ICESat/GLAS group for their hard work in creating this extraordinary data set. We would also like to thank Chris Shuman and Kris Barbieri for their help in interpreting the GLAS data. Useful comments from Ian Folkins, Steve Sherwood, and Courtney Schumacher are gratefully acknowledged. This work was supported by NASA EOS/IDS and ACMAP grants, both to Texas A&M University.

References

Alcala, C. M., and A. E. Dessler (2002), Observations of deep convection in the tropics using the Tropical Rainfall Measuring Mission (TRMM) precipitation radar, *J. Geophys. Res.*, *107*(D24), 4792, doi:10.1029/2002JD002457.

Atticks, M. G., and G. D. Robinson (1983), Some features of the structure of the tropical tropopause, *Q. J. R. Meteorol. Soc.*, *109*, 295–308.

Bergman, J. W., and M. L. Salby (1996), Diurnal variations of cloud cover and their relationship to climatological conditions, *J. Clim.*, *9*, 2802–2820.

Dessler, A. E. (2000), *The Chemistry and Physics of Stratospheric Ozone*, 214 pp., Elsevier, New York.

Dessler, A. E. (2002), The effect of deep, tropical convection on the tropical tropopause layer, *J. Geophys. Res.*, *107*(D3), 4033, doi:10.1029/2001JD000511.

Dessler, A. E., S. P. Palm, W. D. Hart, and J. D. Spinhirne (2006), Tropopause-level thin cirrus coverage revealed by ICESat/Geoscience Laser Altimeter System, *J. Geophys. Res.*, *111*, D08203, doi:10.1029/2005JD006586.

Duda, D. P., J. D. Spinhirne, and E. W. Eloranta (2001), Atmospheric multiple scattering effects on GLAS altimetry, part I, Calculations of single-pulse bias, *IEEE Trans. Geosci. Remote Sens.*, *39*, 92–101.

Folkins, I., and R. V. Martin (2005), The vertical structure of tropical convection, and its impact on the budgets of water vapor and ozone, *J. Atmos. Sci.*, *62*, 1560–1573.

Folkins, I., M. Loewenstein, J. Podolske, S. J. Oltmans, and M. Proffitt (1999), A 14 km mixing barrier in the tropics: Evidence from ozonesondes and aircraft measurements, *J. Geophys. Res.*, *104*, 22,095–22,102.

Folkins, I., C. Braun, A. M. Thompson, and J. Witte (2002), Tropical ozone as an indicator of deep convection, *J. Geophys. Res.*, *107*(D13), 4184, doi:10.1029/2001JD001178.

Gettelman, A., W. J. Randel, F. Wu, and S. T. Massie (2002a), Transport of water vapor in the tropical tropopause layer, *Geophys. Res. Lett.*, *29*(1), 1009, doi:10.1029/2001GL013818.

Gettelman, A., M. L. Salby, and F. Sassi (2002b), Distribution and influence of convection in the tropical tropopause region, *J. Geophys. Res.*, *107*(D10), 4080, doi:10.1029/2001JD001048.

Gettelman, A., P. M. D. Forster, M. Fujiwara, Q. Fu, H. Vomel, L. K. Gohar, C. Johanson, and M. Ammerman (2004), Radiation balance of the tropical tropopause layer, *J. Geophys. Res.*, *109*, D07103, doi:10.1029/2003JD004190.

Hart, W. D., J. D. Spinhirne, S. P. Palm, and D. L. Hlavka (2005), Height distribution between cloud and aerosol layers in the Indian Ocean region from the GLAS spaceborne lidar, *Geophys. Res. Lett.*, *32*, L22S06, doi:10.1029/2005GL023671.

Hartmann, D. L., J. R. Holton, and Q. Fu (2001), The heat balance of the tropical tropopause, cirrus, and stratospheric dehydration, *Geophys. Res. Lett.*, *28*, 1969–1972.

Heymsfield, A. J., and G. M. McFarquhar (1996), High albedos of cirrus in the tropical pacific warm pool: Microphysical interpretations from CEPEX and from Kwajalein, Marshall Islands, *J. Atmos. Sci.*, *53*, 2424–2451.

Heymsfield, G. M., R. Fulton, and J. D. Spinhirne (1991), Aircraft overflight measurements of midwest severe storms: Implications on geosynchronous satellite interpretations, *Mon. Weather Rev.*, *119*, 436–456.

Highwood, E. J., and B. J. Hoskins (1998), The tropical tropopause, *Q. J. R. Meteorol. Soc.*, *124*, 1579–1604.

Hlavka, D. L., S. P. Palm, W. D. Hart, J. D. Spinhirne, M. J. McGill, and E. J. Welton (2005), Aerosol and cloud optical depth from GLAS: Results and verifications for an October 2003 California fire smoke case, *Geophys. Res. Lett.*, *32*, L22S07, doi:10.1029/2005GL023413.

Holton, J. R., and A. Gettelman (2001), Horizontal transport and the dehydration of the stratosphere, *Geophys. Res. Lett.*, *28*, 2799–2802.

Holton, J. R., P. H. Haynes, M. E. McIntyre, A. R. Douglass, R. B. Rood, and L. Pfister (1995), Stratosphere-troposphere exchange, *Rev. Geophys.*, *33*, 403–439.

Jensen, E. J., and L. Pfister (2004), Transport and freeze-drying in the tropical tropopause layer, *J. Geophys. Res.*, *109*, D02207, doi:10.1029/2003JD004022.

Jensen, E. J., O. B. Toon, H. B. Selkirk, J. D. Spinhirne, and M. R. Schoeberl (1996), On the formation and persistence of subvisible cirrus clouds near the tropical tropopause, *J. Geophys. Res.*, *101*, 21,361–21,375.

Johnson, R. H., T. M. Rickenbach, S. A. Rutledge, P. E. Ciesielski, and W. H. Schubert (1999), Trimodal characteristics of tropical convection, *J. Clim.*, *12*, 2397–2418.

Liao, X., W. B. Rossow, and D. Rind (1995), Comparison between SAGE II and ISCCP high-level clouds, 1, Global and zonal mean cloud amounts, *J. Geophys. Res.*, *100*, 1121–1135.

Liebmann, B., and C. A. Smith (1996), Description of a complete (interpolated) outgoing longwave radiation data set, *Bull. Am. Meteorol. Soc.*, *77*, 1275–1277.

Liu, C., and E. J. Zipser (2005), Global distribution of convection penetrating the tropical tropopause, *J. Geophys. Res.*, *110*, D23104, doi:10.1029/2005JD006063.

Luo, B. P., et al. (2003), Dehydration potential of ultrathin clouds at the tropical tropopause, *Geophys. Res. Lett.*, *30*(11), 1557, doi:10.1029/2002GL016737.

McFarquhar, G. M., A. J. Heymsfield, J. Spinhirne, and B. Hart (2000), Thin and subvisual tropopause tropical cirrus: Observations and radiative impacts, *J. Atmos. Sci.*, *57*, 1841–1853.

McGill, M. J., L. Li, W. D. Hart, G. M. Heymsfield, D. L. Hlavka, P. E. Racette, L. Tian, M. A. Vaughan, and D. M. Winker (2004), Combined lidar-radar remote sensing: Initial results from CRYSTAL-FACE, *J. Geophys. Res.*, *109*, D07203, doi:10.1029/2003JD004030.

Nesbitt, S. W., and E. J. Zipser (2003), The diurnal cycle of rainfall and convective intensity according to three years of TRMM measurements, *J. Clim.*, *16*, 1456–1475.

Norris, J. R. (1998), Low cloud type over the ocean from surface observations, part II, Geographical and seasonal variations, *J. Clim.*, *11*, 383–403.

Palm, S., W. Hart, D. Hlavka, E. J. Welton, A. Mahesh, and J. Spinhirne (2002), Geosciences Laser Altimeter System (GLAS) atmospheric data products, algorithm theoretical basis document, version 4.2, pp. 137, NASA Goddard Space Flight Center, Greenbelt, Md.

Randel, W. J., F. Wu, and D. J. Gaffen (2000), Interannual variability of the tropical tropopause derived from radiosonde data and NCEP reanalysis, *J. Geophys. Res.*, *105*, 15,509–15,523.

Seidel, D. J., M. Free, and J. Wang (2005), Diurnal cycle of upper-air temperature estimated from radiosondes, *J. Geophys. Res.*, *110*, D09102, doi:10.1029/2004JD005526.

Sherwood, S. C., and A. E. Dessler (2000), On the control of stratospheric humidity, *Geophys. Res. Lett.*, *27*, 2513–2516.

Sherwood, S. C., and A. E. Dessler (2001), A model for transport across the tropical tropopause, *J. Atmos. Sci.*, *58*, 765–779.

Sherwood, S. C., J.-H. Chae, P. Minnis, and M. McGill (2004), Underestimation of deep convective cloud tops by thermal imagery, *Geophys. Res. Lett.*, *31*, L11102, doi:10.1029/2004GL019699.

Spinhirne, J. D., and W. D. Hart (1990), Cirrus structure and radiative parameters from the airborne lidar and spectral radiometer observations: The 28 October 1986 FIRE study, *Mon. Weather Rev.*, *118*, 2329–2343.

Spinhirne, J. D., S. P. Palm, W. D. Hart, D. L. Hlavka, and E. J. Welton (2005), Cloud and aerosol measurements from GLAS: Overview and initial results, *Geophys. Res. Lett.*, *32*, L22S03, doi:10.1029/2005GL023507.

Swinbank, R., and A. O'Neill (1994), A stratosphere-troposphere data assimilation system, *Mon. Weather Rev.*, *122*, 686–702.

Wang, P.-H., M. P. McCormick, P. Minnis, G. S. Kent, G. K. Yue, and K. M. Skeens (1995), A method for estimating vertical distribution of the SAGE II opaque cloud frequency, *Geophys. Res. Lett.*, *22*, 243–246.

Wang, P. H., P. Minnis, M. P. McCormick, G. S. Kent, and K. M. Skeens (1996), A 6–year climatology of cloud occurrence frequency from stratospheric aerosol and gas experiment II observations (1985–1990), *J. Geophys. Res.*, *101*, 29,407–29,429.

Winker, D. M., and C. R. Trepte (1998), Laminar cirrus observed near the tropical tropopause by LITE, *Geophys. Res. Lett.*, *25*, 3351–3354.

Wylie, D. P., and W. P. Menzel (1989), Two years of cloud cover statistics using VAS, *J. Clim.*, *2*, 380–392.

Wylie, D. P., and W. P. Menzel (1999), Eight years of high cloud statistics using HIRS, *J. Clim.*, *12*, 170–184.

Wylie, D. P., and H. M. Woolf (2002), The diurnal cycle of upper-tropospheric clouds measured by GOES-VAS and the ISCCP, *Mon. Weather Rev.*, *130*, 171–179.

Yang, G. Y., and J. Slingo (2001), The diurnal cycle in the Tropics, *Mon. Weather Rev.*, *129*, 784–801.

Zwally, H. J., et al. (2002), ICESat's laser measurements of polar ice, atmosphere, ocean, and land, *Geodynamics*, *34*, 405–445.

A. E. Dessler, Department of Atmospheric Sciences, Texas A&M University, TAMU 3150, College Station, TX 77843, USA. (adessler@tamu.edu)

S. P. Palm, Science Systems and Applications Inc., Lanham, MD 20706, USA.

J. D. Spinhirne, NASA Goddard Space Flight Center, Greenbelt, MD 20771, USA.